



Research Article

Gloria Rita Argento*, Stefano Gabriele, Luciano Teresi, and Valerio Varano

Target metric and Shell Shaping**

<https://doi.org/10.1515/cls-2021-0002>

Received Sep 16, 2020; accepted Nov 15, 2020

Abstract: We exploit the possibility of deforming a shell by assigning a target metric, which, for 2D structures, is decomposed into the first and second target fundamental-forms. As well known, an elastic shell may change its shape under two different kinds of actions: one are the loadings, the other one are the distortions, also known as the pre-strains. Actually, the target fundamental forms prescribe a sought shape for the solid, and the metric effectively realized is the one that minimizes the distance, measured through an elastic energy, between the target and the actual fundamental forms. The proposed method is very effective in deforming shells.

Keywords: shell, elastic metric, distortions, non linear elasticity, target metric

1 Introduction: shape and change in shape in a nutshell

The problem of the shape reconstruction from local geometrical properties, such as the metric or the curvature, is common to different fields, among them are Shape Analysis, Computer Graphics [1, 2] and Solid Mechanics [3, 4].

In the last years, the concepts of *target metric*, *non-euclidean plates* [5] and *non-linear distortions* [6], have been widely used to describe shape formation processes in both natural (e.g. growth and remodeling of biological structures), and artificial contexts (e.g. design of actuators). In particular, the local strain, in the deformation of a solid

body (or a shell), can be characterized by the change of metric and curvature [7, 8].

Deformations in engineering structures are generally studied according to the effect of loadings, assuming both small or large displacements. Other causes of deformation and stress in structures are the distortions, for example, the thermal distortions. The effects of distortions are usually studied in small displacement regime, and few studies tackle the problem of large distortions that can yield large deformations; even more interesting are the cases where distortions induce large shape changes without stressing the structure. This last phenomenon is typical of biological structures [9]. In this work we investigate the morphing of elastic shell-like structures, with a view towards engineering and architectural problems.

Our aim is to morph a material body basing on the theory of finite elasticity with large distortions, *i.e.* an assigned distortion induces a target metric and the configuration which is actually realized is the one that minimizes the distance, measured through the elastic energy, between the target metric and the actual one.

In order to do that, it is very important to recall some key concepts, which cross all the aforementioned fields, and which concern, in general, geometric issues.

The fundamental concept is that of *differentiable manifold*, that is, of parametrized geometry, a natural extension of the concept of parametric surface.

In the simplest case, the parameterization of a geometric object living in Euclidean space occurs through a map which, by establishing a correspondence between a region of \mathbb{R}^N (where N is 2 for two-dimensional bodies and 3 for three-dimensional bodies) and a region of the Euclidean space \mathcal{E} (the geometric object), allows the user to “move” inside the considered object, or to identify, through the coordinates, any point of the object itself.

A geometric object, embedded in three-dimensional Euclidean space, can be three-dimensional or two-dimensional, depending on the number of coordinates needed to describe it.

We can refer to parametric surfaces as two-dimensional objects and to parametric solids as three-dimensional objects.

Object parameterization is a differentiable function f from \mathbb{R}^2 to \mathcal{E} , for a surface, and from \mathbb{R}^3 to \mathcal{E} , for a solid. In

*Corresponding Author: Gloria Rita Argento: Department of Architecture, Roma Tre University, Rome, Italy;
Email: gloriarita.argento@uniroma3.it

Stefano Gabriele, Valerio Varano: Department of Architecture, Roma Tre University, Rome, Italy

Luciano Teresi: Department of Mathematics and Physics, Roma Tre University, Rome, Italy

** Paper included in the Special Issue entitled: Shell and Spatial Structures: Between New Developments and Historical Aspects

both cases the output of the function are the 3 coordinates (x, y, z) that identify a point in the Euclidean space. For this reason, we can say that the function f provides a global description of the object.

From a geometric point of view it is very important to introduce a local description, namely, the one that describes the geometry of the neighborhood of a considered point. This description is made through the tangent map ∇f , being ∇ the gradient operator.

The distinction between global and local description of the shape of an object is very important. The shape of an object can be described through a (regular) function f up to a rigid transformation (global isometry), which has Euclidean space as its codomain, and a two-dimensional \mathbb{R}^N region as its domain (surfaces: $N = 2$) or three-dimensional (solid: $N = 3$). The local description gives the shape of the neighborhood of a point of the object. Given a global description it is possible to obtain, by differentiation, the local description.

In the geometry of surfaces their local description is given by the first fundamental form A (metric of the surface) and by the second fundamental form B (curvature of the surface). In simple terms the metric describes how an infinitesimal element of surface is shaped, while the curvature describes how an infinitesimal element is rotated with respect to the immediately adjacent infinitesimal elements.

An important result from the differential geometry is that assigning the fields A and B , corresponding to a local description, and provided that these fields respect the so-called *compatibility equations* (Gauss and Mainardi-Codazzi), it is then possible to obtain the global geometry of a surface by integration [7].

This also means that by locally changing the metric and curvature of a surface, it is possible to change its overall geometry.

This principle is continuously exploited in nature in particular in 2 contexts: *growth* and *active deformation*. In the first case, the global geometry is determined by adding new material and re-organizing the existing one at a local level. Let us think of the case of the growth of a tree that develops its trunk in such a way as to reach the sunlight. On the other hand a simple example of active deformation is that of muscle activation: to move a hand towards an object (global displacement) a contraction of the arm's muscles (local shape change) is needed.

In Mechanics the introduced purely geometric facts are then related to elasticity and, in this context, we do not speak simply about geometrical objects, but we speak about *bodies*. A body is a differentiable manifold which, at any time, fill a given configuration in the Euclidean space. A motion is a sequence of configurations parametrized by

the time, and is described by a map f_t , which associate a configuration in the space \mathcal{E} for each instant t . Elasticity is the phenomenon whereby a body, locally, tends to prefer one shape rather than another. The preferred configuration of a body is generally associated with a reference configuration, or initial configuration, otherwise known as the rest configuration. In that configuration the body is not subjected to internal stresses. When, due to external causes (for example a load), the body moves from the rest configuration then elastic energy accumulates in every point of the body. The elastic energy is a function that gauges the elastic strain (also known as elastic metric).

The elastic strain is the difference (calculated in some linear or non-linear way) between the local shape (metric and/or curvature) in the current configuration and the local shape in the rest configuration (target metric and target curvature). The global configuration that will take place will be the one that minimize the total potential energy, given by the elastic energy minus the potential energy of the loads. Therefore, in the absence of loads, the body will tend to return to its rest configuration.

A different case is when so-called inelastic deformations (thermal expansion, swelling, plasticity) are present, where the target metric (curvature) is no longer associated with the reference configuration or, more in general, with a global configuration, but is locally assigned in the body. If the assigned target metric respects the compatibility equations, above recalled, and it is compatible with some given boundary conditions, then it will be possible to realize a global configuration (target configuration), whose local form corresponds to the target metric. In absence of loads the body will assume the target configuration, which will be free of internal stresses. If the target metric does not respect the compatibility equations or the compatibility with the boundary conditions, no target configuration exists and, in the absence of loads, the body will arrange itself in a configuration which will be as locally as possible similar to the elastic metric, in order to minimize the elastic energy. Within this configuration internally self-balanced stresses are present, named self-stresses.

In summary, to generate a change in shape of an object it is possible to follow at least two paths:

1. applying a load (potential energy of the loads: global), generating as a response an elastic energy and, consequently, local deformations and tensions.
2. assigning a local shape change (pre-strain) and obtaining a global shape change, which can be stress-free (if the target metric is compatible) or having self-stresses (if the target metric is not compatible).

In recent years an interesting topic that involves shell-like structures is the Form-Finding (FF) [10], where an optimal structural form is searched for minimizing the contribution of the bending moments in its mechanical behavior. This means that an architectural shell can be shaped, according to certain load and boundary conditions, to carry design loads only by exploiting membrane forces. Form-Finding methods are generally based on equilibrium conditions to be satisfied in the actual configuration (namely force methods). What here proposed could be also interesting to reformulate new FF methods based on target metric assignment, where compatibility conditions could integrate or substitute the force conditions given in the classical FF. A very recent example shows how a discrete change in the metric of the surface of a wooden pavilion, made of assembled panels, is the tool used to design its target shape [11]. We will show how, in order to obtain a configuration very different from the initial is more easy, from a computational point of view, to assign local strains instead of loads.

The paper is hence structured as in the following. In Section 2 we give an introduction of distortions and the elastic metric for 3D elasticity. These concepts will be specified for a 2D shell-like body in Section 3, where also the elastic Fundamental Forms will be derived. In Section 4 some numerical examples of shell morphing will be presented considering both initially flat and curved shell-like bodies. Finally the Conclusions will be followed by an appendix devoted to the nonlinear shell model used in this work.

2 3D Distortions and the elastic metric

We give a short introduction of the notion of distortions and the associated elastic metric [6]. Given a reference configuration $\mathcal{B}_{\bar{y}}$ of a 3D body, we define a new configuration \mathcal{B}_y via the map f :

$$f : \mathcal{B}_{\bar{y}} \rightarrow \mathcal{E} \quad (1)$$

$$\bar{y} \mapsto y = f(\bar{y}), \quad (2)$$

where \mathcal{E} is the 3D Euclidean ambient space; the gradient $\mathbf{F} = \nabla f$ is the tangent map from the tangent bundle $T\mathcal{B}_{\bar{y}}$ of $\mathcal{B}_{\bar{y}}$, to the tangent bundle $T\mathcal{B}_y$ of \mathcal{B}_y . *Distortions* are described by a smooth tensor-valued field

$$\mathbf{F}_o : \bar{Y} \rightarrow \text{Lin}(T\mathcal{B}_{\bar{y}}, T\mathcal{B}_{\bar{y}}), \quad (3)$$

with $\text{Lin}(T\mathcal{B}_{\bar{y}}, T\mathcal{B}_{\bar{y}})$ an endomorphism of $T\mathcal{B}_{\bar{y}}$, with $J_o := \det \mathbf{F}_o > 0$. The key distinction between a distortion \mathbf{F}_o and

the gradient of a deformation \mathbf{F} can be briefly summarized as follows: \mathbf{F} embeds body elements onto \mathcal{E} ; conversely, \mathbf{F}_o is not required to be the gradient of any map, and in general it does not exist an embedding for the distorted body elements, that is \mathbf{F}_o is not *compatible*. The extra strain that must be added to \mathbf{F}_o is called *elastic strain*, a notion put forward in [12, 13] to tell the difference between elastic and plastic strains

$$\mathbf{F}_e = \mathbf{F} \mathbf{F}_o^{-1}, \quad (4)$$

The three tangent maps \mathbf{F} , \mathbf{F}_o , and \mathbf{F}_e (see Figure 1), prompt the definition of the following metric tensors, having the role of right Cauchy-Green strain-measures:

$$\mathbf{C}_o = \mathbf{F}_o^T \mathbf{F}_o, \quad \text{target metric, due to } \mathbf{F}_o, \quad (5)$$

$$\mathbf{C} = \mathbf{F}^T \mathbf{F}, \quad \text{actual metric, given by } \mathbf{F},$$

$$\mathbf{C}_e = \mathbf{F}_e^T \mathbf{F}_e = \mathbf{F}_o^{-T} \mathbf{C} \mathbf{F}_o^{-1} \quad \text{elastic metric.}$$

The name *target metric*, also known as natural or intrinsic metric [14], stems from the fact that, in order to get a minimum of the elastic energy, the actual metric \mathbf{C} will be as close as possible, in the energy norm, to the target one; in particular, if \mathbf{C} is equal to \mathbf{C}_o , then the elastic metric is trivial: $\mathbf{C} = \mathbf{C}_o \Leftrightarrow \mathbf{C}_e = \mathbf{I}$. In general, \mathbf{C}_o is not Euclidean, i.e., it does not exist any embedding compatible with \mathbf{C}_o , and the actual configuration will have $\mathbf{C}_e \neq \mathbf{I}$.

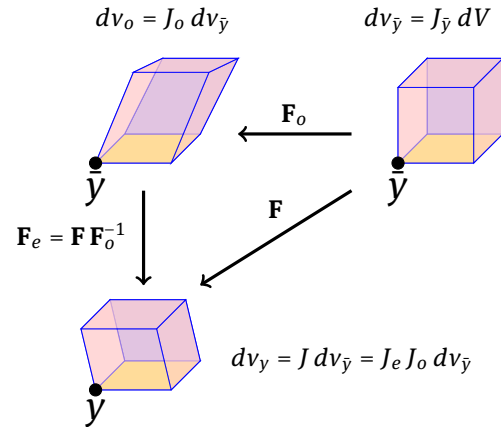


Figure 1: The essence of a distortion. The volume element $dv_{\bar{y}}$, attached to a point $\bar{y} \in \mathcal{B}_{\bar{y}}$ of the source configuration (top, right) is mapped by \mathbf{F}_o onto a distorted element dv_o , attached to the same point \bar{y} (top, left). To get a compatible volume element dv_y (bottom, left), we must add a further strain to \mathbf{F}_o , called the elastic strain \mathbf{F}_e . The embedding \mathbf{F} is thus given by $\mathbf{F} = \mathbf{F}_e \mathbf{F}_o$.

3 2D Distortions and the elastic fundamental forms

3.1 The representation of the metric tensor for shell-like bodies

Let $\{o; \mathbf{c}_1, \mathbf{c}_2, \mathbf{c}_3\}$ be an orthonormal frame of \mathcal{E} ; to denote the Cartesian components, we shall use the subscripts $\alpha, \beta = 1, 2$ and $i, j = 1, 2, 3$. We define a *shell-like domain* as a flat 3D volume $\mathcal{S} = Z \times H$, the Cartesian product of $Z \in \text{span}(\mathbf{c}_1, \mathbf{c}_2)$, and $H \in \text{span}(\mathbf{c}_3)$, whose characteristic diameter is much larger than the thickness H : $\sqrt{\text{area}(Z)}/H \gg 1$. A point of \mathcal{S} is represented by the three coordinates (z_1, z_2, ζ) . Following [15], we define a *shell-like body* as the 3D volume f_k extruded from the surfaces \hat{f}_k , with $k = \bar{y}, y$, along their normals \mathbf{n}_k

$$\begin{aligned} f_k : \mathcal{S} &\rightarrow \mathcal{E}, \\ \text{with } f_k(z_1, z_2, \zeta) &= \hat{f}_k(z_1, z_2) + \zeta \mathbf{n}_k(z_1, z_2), \end{aligned} \quad (6)$$

We always consider a reference surface $\hat{f}_{\bar{y}}$ and an actual surface \hat{f}_y , the unknown of our problem. The tangent vectors $\mathbf{a}_{k\alpha}$ to the surfaces \hat{f}_k , and the surface normals \mathbf{n}_k , are defined in terms of the partial derivatives of \hat{f}_k :

$$\mathbf{a}_{k\alpha} = \hat{f}_{k,\alpha} = \partial \hat{f}_k / \partial z_\alpha; \quad \mathbf{n}_k = \frac{\mathbf{a}_{k1} \times \mathbf{a}_{k2}}{\|\mathbf{a}_{k1} \times \mathbf{a}_{k2}\|}. \quad (7)$$

Given (6), its gradient $\mathbf{F}_k = \nabla f_k$ is represented by

$$\mathbf{F}_k = \hat{\mathbf{F}}_k + \mathbf{n}_k \otimes \mathbf{e}_3 + \zeta \nabla \mathbf{n}_k, \quad \text{with } \hat{\mathbf{F}}_k = \nabla \hat{f}_k. \quad (8)$$

The matrix-like representation $[\mathbf{F}_k]$ of \mathbf{F}_k is given by

$$\begin{aligned} [\mathbf{F}_k] &= [\mathbf{a}_{k1} \mid \mathbf{a}_{k2} \mid \mathbf{n}_k] + \zeta [\mathbf{n}_{k,1} \mid \mathbf{n}_{k,2} \mid 0] \\ &= \begin{bmatrix} \hat{f}_{k1,1} & \hat{f}_{k1,2} & n_{k1} \\ \hat{f}_{k2,1} & \hat{f}_{k2,2} & n_{k2} \\ \hat{f}_{k3,1} & \hat{f}_{k3,2} & n_{k3} \end{bmatrix} + \zeta \begin{bmatrix} n_{1,1} & n_{1,2} & 0 \\ n_{2,1} & n_{2,2} & 0 \\ n_{3,1} & n_{3,2} & 0 \end{bmatrix} \end{aligned} \quad (9)$$

with $\hat{f}_{ki} = \hat{f}_k \cdot \mathbf{c}_i$, and $n_{ki} = \mathbf{n}_k \cdot \mathbf{c}_i$ the Cartesian components of \hat{f}_k , \mathbf{n}_k , respectively. Given (8), the associated metric \mathbf{C}_k can be written in terms of the surface *Fundamental Forms* (FFs) by

$$\mathbf{C}_k = \mathbf{F}_k^T \mathbf{F}_k = \mathbf{U}_k^2 \doteq \mathbf{A}_k + 2 \zeta \mathbf{B}_k, \quad (10)$$

where \mathbf{U}_k is the right stretch tensor associated to polar decomposition of \mathbf{F}_k , and

$$\mathbf{A}_k = \hat{\mathbf{F}}_k^T \hat{\mathbf{F}}_k, \quad \mathbf{B}_k = \frac{1}{2} \left(\hat{\mathbf{F}}_k^T \nabla \mathbf{n}_k + \nabla \mathbf{n}_k^T \hat{\mathbf{F}}_k \right), \quad (11)$$

are the first and the second fundamental forms, respectively. We note that the other summands in $\mathbf{F}_k^T \mathbf{F}_k$ contain a term

quadratic in ζ , which is neglected, plus a term which is constant, that is $\mathbf{e}_3 \otimes \mathbf{e}_3$, and finally the term

$$\hat{\mathbf{F}}_k^T (\mathbf{n}_k \otimes \mathbf{e}_3) + (\mathbf{e}_3 \otimes \mathbf{n}_k) \hat{\mathbf{F}}_k = \mathbf{0}, \quad (12)$$

which is null, being $\mathbf{a}_{k\alpha} \perp \mathbf{n}_k$. The matrix-like representation of \mathbf{C}_k is given by

$$\begin{aligned} [\mathbf{C}_k] &\doteq \left[\begin{array}{cc|c} \mathbf{a}_{k1} \cdot \mathbf{a}_{k1} & \mathbf{a}_{k1} \cdot \mathbf{a}_{k2} & 0 \\ \mathbf{a}_{k1} \cdot \mathbf{a}_{k2} & \mathbf{a}_{k2} \cdot \mathbf{a}_{k2} & 0 \\ \hline 0 & 0 & 1 \end{array} \right] \\ + 2 \zeta &\left[\begin{array}{cc|c} \mathbf{a}_{k1} \cdot \mathbf{n}_{k,1} & \mathbf{a}_{k1} \cdot \mathbf{n}_{k,2} + \mathbf{n}_{k,1} \cdot \mathbf{a}_{k2} & 0 \\ \mathbf{a}_{k1} \cdot \mathbf{n}_{k,2} + \mathbf{n}_{k,1} \cdot \mathbf{a}_{k2} & \mathbf{a}_{k2} \cdot \mathbf{n}_{k,2} & 0 \\ \hline 0 & 0 & 0 \end{array} \right] \end{aligned} \quad (13)$$

Following the linear representation of \mathbf{C}_k , see (10), we assume a similar linear representation for the right stretch \mathbf{U}_k :

$$\mathbf{U}_k \doteq \mathbf{U}_{k0} + \zeta \mathbf{U}_{k1}, \quad (14)$$

Using (14), we can represent \mathbf{C}_k in terms of \mathbf{U}_{k0} and \mathbf{U}_{k1} ; as previously done for (10), we neglect the quadratic terms, and write

$$\begin{aligned} \mathbf{C}_k &= (\mathbf{U}_{k0} + \zeta \mathbf{U}_{k1})^2 \doteq \mathbf{U}_{k0}^2 + 2 \zeta \text{sym}(\mathbf{U}_{k0} \mathbf{U}_{k1}) \\ &= \mathbf{A}_k + 2 \zeta \mathbf{B}_k; \end{aligned} \quad (15)$$

it follows a relation between the 3D stretches \mathbf{U}_{k0} , \mathbf{U}_{k1} and the 2D FFs \mathbf{A}_k , \mathbf{B}_k :

$$\mathbf{U}_{k0}, \mathbf{U}_{k1} \Rightarrow \mathbf{A}_k = \mathbf{U}_{k0}^2, \quad \mathbf{B}_k = \text{sym}(\mathbf{U}_{k0} \mathbf{U}_{k1}); \quad (16)$$

$$\mathbf{A}_k, \mathbf{B}_k \Rightarrow \mathbf{U}_{k0} = \sqrt{\mathbf{A}_k}, \quad (17)$$

$$\mathbf{U}_{k1} = \frac{1}{\text{tr}(\mathbf{U}_{k0})} \left(\mathbf{B}_k + \det(\mathbf{U}_{k0}) \mathbf{U}_{k0}^{-1} \mathbf{B}_k \mathbf{U}_{k0}^{-1} \right);$$

The equation (17)₂ is the solution for \mathbf{U}_{k1} of (16)₂. In the following, we shall also need the linear expansion of the inverse of \mathbf{U}_k ; from (14), we have

$$\mathbf{U}_k^{-1} \doteq \mathbf{U}_{k0}^{-1} - \zeta \mathbf{D}_k, \quad \text{with } \mathbf{D}_k = \mathbf{U}_{k0}^{-1} \mathbf{U}_{k1} \mathbf{U}_{k0}^{-1}. \quad (18)$$

The relative metric $\mathbf{C}_{\bar{y}y}$ of \hat{f}_y with respect to $\hat{f}_{\bar{y}}$ is given by $\mathbf{C}_{\bar{y}y} = (\mathbf{U}_{\bar{y}}^{-1} \mathbf{U}_y) (\mathbf{U}_{\bar{y}}^{-1} \mathbf{U}_y)^T$; from (10, 18), we have

$$\begin{aligned} \mathbf{C}_{\bar{y}y} &= (\mathbf{U}_{\bar{y}}^{-1} \mathbf{U}_y) (\mathbf{U}_{\bar{y}}^{-1} \mathbf{U}_y)^T = \mathbf{U}_{\bar{y}}^{-1} \mathbf{C}_y \mathbf{U}_{\bar{y}}^{-1} \\ &= (\mathbf{U}_{\bar{y}0}^{-1} - \zeta \mathbf{D}_{\bar{y}}) (\mathbf{A}_y + 2 \zeta \mathbf{B}_y) (\mathbf{U}_{\bar{y}0}^{-1} - \zeta \mathbf{D}_{\bar{y}}) \\ &= \mathbf{U}_{\bar{y}0}^{-1} \mathbf{A}_y \mathbf{U}_{\bar{y}0}^{-1} + 2 \zeta \mathbf{U}_{\bar{y}0}^{-1} \left(\mathbf{B}_y - \text{sym}(\mathbf{A}_y \mathbf{U}_{\bar{y}0}^{-1} \mathbf{U}_{\bar{y}1}) \right) \mathbf{U}_{\bar{y}0}^{-1} \\ &\quad + o(\zeta) \\ &\doteq \mathbf{A}_{\bar{y}y} + 2 \zeta \mathbf{B}_{\bar{y}y}. \end{aligned} \quad (19)$$

It follows a representation formula for the relative FFs of \hat{f}_y with respect to $\hat{f}_{\bar{y}}$

$$\mathbf{A}_{\bar{y}y} = \mathbf{U}_{\bar{y}0}^{-1} \mathbf{A}_y \mathbf{U}_{\bar{y}0}^{-1}, \quad (20)$$

$$\mathbf{B}_{\bar{y}y} = \mathbf{U}_{\bar{y}0}^{-1} \left(\mathbf{B}_y - \text{sym}(\mathbf{A}_y \mathbf{U}_{\bar{y}0}^{-1} \mathbf{U}_{\bar{y}1}) \right) \mathbf{U}_{\bar{y}0}^{-1}.$$

3.2 The representation of the target metric for shell-like bodies

Given (9), we assume the following representation for a distortion \mathbf{F}_o to be used for shell-like bodies

$$|\mathbf{F}_o| = [\mathbf{a}_{o1} | \mathbf{a}_{o2} | \mathbf{d}_o] + \zeta [\mathbf{d}_{o,1} | \mathbf{n}_{o,2} | 0], \quad (21)$$

with the key difference that the field \mathbf{d}_o , with $|\mathbf{d}_o| = 1$, can be in general independent from the two fields $\mathbf{a}_{o\alpha}$. Here, we are interested in developing a Kirchhoff-like shell model, and we assume $\mathbf{d}_o \perp \mathbf{a}_{o\alpha}$. From (21), and the orthogonality between \mathbf{d}_o and $\mathbf{a}_{o\alpha}$, we can define a 3D target metric \mathbf{C}_o which includes the target FFs \mathbf{A}_o and \mathbf{B}_o

$$\mathbf{C}_o = \mathbf{F}_o^T \mathbf{F}_o = \mathbf{U}_o^2 = \mathbf{A}_o + 2 \zeta \mathbf{B}_o + o(\zeta), \quad (22)$$

where \mathbf{U}_o is the right stretch tensor associated to polar decomposition of \mathbf{F}_o , and

$$\mathbf{A}_o = \hat{\mathbf{F}}_o^T \hat{\mathbf{F}}_o, \quad \mathbf{B}_o = \frac{1}{2} \left(\hat{\mathbf{F}}_o^T \nabla \mathbf{d}_o + \nabla \mathbf{d}_o^T \hat{\mathbf{F}}_o \right). \quad (23)$$

The matrix-like representation of \mathbf{C}_o is given by

$$|\mathbf{C}_o| \doteq \begin{bmatrix} \mathbf{a}_{o1} \cdot \mathbf{a}_{o1} & \mathbf{a}_{o1} \cdot \mathbf{a}_{o2} & 0 \\ \mathbf{a}_{o1} \cdot \mathbf{a}_{o2} & \mathbf{a}_{o2} \cdot \mathbf{a}_{o2} & 0 \\ 0 & 0 & 1 \end{bmatrix} \quad (24)$$

$$+ 2 \zeta \begin{bmatrix} \mathbf{a}_{o1} \cdot \mathbf{d}_{o,1} & \mathbf{a}_{o1} \cdot \mathbf{d}_{o,2} + \mathbf{d}_{o,1} \cdot \mathbf{a}_{o2} & 0 \\ \mathbf{a}_{o1} \cdot \mathbf{d}_{o,2} + \mathbf{d}_{o,1} \cdot \mathbf{a}_{o2} & \mathbf{a}_{o2} \cdot \mathbf{d}_{o,2} & 0 \\ 0 & 0 & 0 \end{bmatrix}$$

As done for \mathbf{U}_k , we also consider a linear expansion of \mathbf{U}_o , and of its inverse \mathbf{U}_o^{-1} ; we have

$$\mathbf{U}_o \doteq \mathbf{U}_{o0} + \zeta \mathbf{U}_{o1}, \quad \mathbf{U}_o^{-1} \doteq \mathbf{U}_{o0}^{-1} - \zeta \mathbf{D}_o, \quad (25)$$

with $\mathbf{D}_o = \mathbf{U}_{o0}^{-1} \mathbf{U}_{o1} \mathbf{U}_{o0}^{-1}$.

Following the same reasoning done with \mathbf{C}_k , see (15, 16, 17), we can write a relation between the 3D target stretches \mathbf{U}_{o0} , \mathbf{U}_{o1} and the 2D target FFs \mathbf{A}_o , \mathbf{B}_o :

$$\mathbf{U}_{o0}, \mathbf{U}_{o1} \Rightarrow \mathbf{A}_o = \mathbf{U}_{o0}^2, \quad \mathbf{B}_o = \text{sym}(\mathbf{U}_{o0} \mathbf{U}_{o1}); \quad (26)$$

$$\mathbf{A}_o, \mathbf{B}_o \Rightarrow \mathbf{U}_{o0} = \sqrt{\mathbf{A}_o}, \quad (27)$$

$$\mathbf{U}_{o1} = \frac{1}{\text{tr}(\mathbf{U}_{o0})} \left(\mathbf{B}_o + \det(\mathbf{U}_{o0}) \mathbf{U}_{o0}^{-1} \mathbf{B}_o \mathbf{U}_{o0}^{-1} \right);$$

3.3 The elastic FFs

The elastic metric (5)₃ for shell-like bodies can be represented as follows

$$\mathbf{C}_e = \mathbf{U}_o^{-1} \mathbf{C}_{\bar{y}\bar{y}} \mathbf{U}_o^{-1}. \quad (28)$$

Following (19), we compute the linear expansion of \mathbf{C}_e ; from (19, 25) we have:

$$\begin{aligned} \mathbf{C}_e &= \mathbf{U}_o^{-1} \mathbf{C}_{\bar{y}\bar{y}} \mathbf{U}_o^{-1} \quad (29) \\ &= (\mathbf{U}_{o0}^{-1} - \zeta \mathbf{D}_o) (\mathbf{A}_{\bar{y}\bar{y}} + 2 \zeta \mathbf{B}_{\bar{y}\bar{y}}) (\mathbf{U}_{o0}^{-1} - \zeta \mathbf{D}_o) \\ &\doteq \mathbf{U}_{o0}^{-1} \left[\mathbf{A}_{\bar{y}\bar{y}} + 2 \zeta (\mathbf{B}_{\bar{y}\bar{y}} - \text{sym}(\mathbf{A}_{\bar{y}\bar{y}} \mathbf{U}_{o0}^{-1} \mathbf{U}_{o1})) \right] \mathbf{U}_{o0}^{-1} \\ &= \mathbf{A}_e + 2 \zeta \mathbf{B}_e. \end{aligned}$$

At this point, we can identify the *elastic FFs* \mathbf{A}_e and \mathbf{B}_e :

$$\mathbf{A}_e = \mathbf{U}_{o0}^{-1} \mathbf{A}_{\bar{y}\bar{y}} \mathbf{U}_{o0}^{-1}, \quad (30)$$

$$\mathbf{B}_e = \mathbf{U}_{o0}^{-1} \left(\mathbf{B}_{\bar{y}\bar{y}} - \text{sym}(\mathbf{A}_{\bar{y}\bar{y}} \mathbf{U}_{o0}^{-1} \mathbf{U}_{o1}) \right) \mathbf{U}_{o0}^{-1}.$$

Using the same procedure, we compute the strain $\mathbf{E}_e = 1/2 (\mathbf{C}_e - \mathbf{I})$; the last equality of (29) yields

$$\mathbf{E}_e = \frac{1}{2} (\mathbf{C}_e - \mathbf{I}) = \frac{1}{2} (\mathbf{A}_e - \mathbf{I} + 2 \zeta \mathbf{B}_e) = \mathbf{E}_{e0} + \zeta \mathbf{E}_{e1} \quad (31)$$

$$\Rightarrow \mathbf{E}_{e0} = \frac{1}{2} (\mathbf{A}_e - \mathbf{I}), \quad \mathbf{E}_{e1} = \mathbf{B}_e.$$

The first equality of (19), together with (25, 29), yield

$$\begin{aligned} \mathbf{E}_e &= \frac{1}{2} (\mathbf{U}_o^{-1} \mathbf{C}_{\bar{y}\bar{y}} \mathbf{U}_o^{-1} - \mathbf{I}) \quad (32) \\ &= \frac{1}{2} (\mathbf{U}_{o0}^{-1} - \zeta \mathbf{D}_o) (\mathbf{A}_{\bar{y}\bar{y}} + 2 \zeta \mathbf{B}_{\bar{y}\bar{y}} - \mathbf{I}) (\mathbf{U}_{o0}^{-1} - \zeta \mathbf{D}_o). \end{aligned}$$

Performing all the computations, it follows

$$\mathbf{E}_{e0} = \frac{1}{2} \mathbf{U}_{o0}^{-1} (\mathbf{A}_{\bar{y}\bar{y}} - \mathbf{A}_o) \mathbf{U}_{o0}^{-1}, \quad (33)$$

$$\mathbf{E}_{e1} = \mathbf{U}_{o0}^{-1} (\mathbf{B}_{\bar{y}\bar{y}} - \mathbf{B}_o - \text{sym}((\mathbf{A}_{\bar{y}\bar{y}} - \mathbf{A}_o) \mathbf{U}_{o0}^{-1} \mathbf{U}_{o1})) \mathbf{U}_{o0}^{-1}.$$

We note that \mathbf{E}_{e0} in (31) and (33) coincide, while \mathbf{B}_e from (30)₂ looks quite different from \mathbf{E}_{e1} in (33)₂; actually, after some manipulations it can be proved that they are the same:

$$\mathbf{B}_e = \mathbf{U}_{o0}^{-1} \left[\mathbf{B}_{\bar{y}\bar{y}} - \text{sym} \left(\mathbf{A}_{\bar{y}\bar{y}} \mathbf{U}_{o0}^{-1} \mathbf{U}_{o1} \right) \right] \mathbf{U}_{o0}^{-1} \quad (34)$$

$$= \mathbf{U}_{o0}^{-1} \left[(\mathbf{B}_{\bar{y}\bar{y}} - \mathbf{B}_o) - \text{sym} \left((\mathbf{A}_{\bar{y}\bar{y}} - \mathbf{A}_o) \mathbf{U}_{o0}^{-1} \mathbf{U}_{o1} \right) \right] \mathbf{U}_{o0}^{-1}$$

The apparent diversity of the representations of \mathbf{B}_e can be worked out by considering that $\mathbf{A}_{o0} = \mathbf{U}_{o0}^2$ and using (26)₂, from which it follows that

$$\text{sym} \left(\mathbf{A}_o \mathbf{U}_{o0}^{-1} \mathbf{U}_{o1} \right) = \text{sym} \left(\mathbf{U}_{o0} \mathbf{U}_{o1} \right) = \mathbf{B}_o. \quad (35)$$

3.4 Some Special cases

We list here some cases of target FFs and their associated elastic FFs:

– $\hat{f}_{\bar{y}}$ is a rigid motion

$$\begin{aligned} \hat{f}_{\bar{y}} = \text{rigid motion} &\Rightarrow \begin{cases} \mathbf{A}_{\bar{y}} = \mathbf{I} \\ \mathbf{B}_{\bar{y}} = \mathbf{O} \end{cases} & (36) \\ &\Rightarrow \begin{cases} \mathbf{U}_{\bar{y}o} = \mathbf{I} \\ \mathbf{U}_{\bar{y}1} = \mathbf{O} \end{cases} \Rightarrow \begin{cases} \mathbf{A}_{\bar{y}y} = \mathbf{A}_y \\ \mathbf{B}_{\bar{y}y} = \mathbf{B}_y \end{cases} \end{aligned}$$

– $\mathbf{A}_o = \mathbf{I}$

$$\begin{aligned} \mathbf{A}_o = \mathbf{I} &\Rightarrow \begin{cases} \mathbf{U}_{o0} = \mathbf{I} \\ \mathbf{U}_{o1} = \mathbf{B}_o \end{cases} & (37) \\ &\Rightarrow \begin{cases} \mathbf{E}_{e0} = \frac{1}{2} (\mathbf{A}_{\bar{y}y} - \mathbf{I}) \\ \mathbf{E}_{e1} = \mathbf{B}_{\bar{y}y} - \text{sym}(\mathbf{A}_{\bar{y}y} \mathbf{B}_o) \end{cases} \end{aligned}$$

– $\mathbf{A}_o = \mathbf{I}$ & $\mathbf{A}_{\bar{y}} = \mathbf{I}$

$$\begin{aligned} \begin{cases} \mathbf{A}_o = \mathbf{I} \\ \mathbf{A}_{\bar{y}} = \mathbf{I} \end{cases} &\Rightarrow \begin{cases} \mathbf{U}_{o0} = \mathbf{I}, & \mathbf{U}_{o1} = \mathbf{B}_o \\ \mathbf{U}_{y0} = \mathbf{I}, & \mathbf{U}_{y1} = \mathbf{B}_y \\ \mathbf{A}_{\bar{y}y} = \mathbf{A}_y \\ \mathbf{B}_{\bar{y}y} = \mathbf{B}_y - \text{sym}(\mathbf{A}_y \mathbf{B}_{\bar{y}}) \end{cases} & (38) \\ &\Rightarrow \begin{cases} \mathbf{E}_{e0} = \frac{1}{2} (\mathbf{A}_y - \mathbf{I}) \\ \mathbf{E}_{e1} = \mathbf{B}_y - \text{sym}(\mathbf{A}_y (\mathbf{B}_{\bar{y}} + \mathbf{B}_o)) \end{cases} \end{aligned}$$

– Second target FF is null

$$\begin{aligned} \mathbf{B}_o = \mathbf{O} &\Rightarrow \begin{cases} \mathbf{U}_{o0} = \sqrt{\mathbf{A}_o} \\ \mathbf{U}_{o1} = \mathbf{O} \end{cases} & (39) \\ &\Rightarrow \begin{cases} \mathbf{E}_{e0} = \frac{1}{2} \mathbf{U}_{o0}^{-1} (\mathbf{A}_{\bar{y}y} - \mathbf{A}_o) \mathbf{U}_{o0}^{-1} \\ \mathbf{E}_{e1} = \mathbf{B}_{\bar{y}y} \end{cases} \end{aligned}$$

4 Worked examples of shell morphing

In this section we present some worked examples of the proposed approach, showing the morphing of a shell induced by a target metric. We use the Nagdhi-shell model presented in the Appendix A; the shell model has been solved with the Finite Element Method (FEM) by implementing our equations system into the software COMSOL Multiphysics. FEM implementation is quite straightforward within the chosen software; in particular, the key steps are the followings: write the weak form of the balance equation (A12); select appropriate shape functions; draw and mesh a 2D computational domain Ω ; run a solver. We note that our implementation requires Ω to be a flat domain, without restriction on its shape. The reference shell is then defined through a map $\hat{f}_{\bar{y}} : \Omega \rightarrow \mathcal{E}$.

Given the orthonormal frame $\{o; \mathbf{c}_1, \mathbf{c}_2, \mathbf{c}_3\}$, in our examples we always consider a rectangular computational domain $Z \in \text{span}(\mathbf{c}_1, \mathbf{c}_2)$, where Z is the region $(z_1, z_2) \in [-L/2, L/2] \times [-W/2, W/2]$ (see Figure 2); the thickness H of the shell-like region is assumed to be $H = L/100$. For the first five examples the ratio L/W has no role; for the last one it is very important, and we set $L/W = 10$.

4.1 Bending at constant stretch (flat reference)

We consider as reference shell $\hat{f}_{\bar{y}}$ a flat domain obtained by a $\pi/4$ rotation of the computational domain. The matrix-like

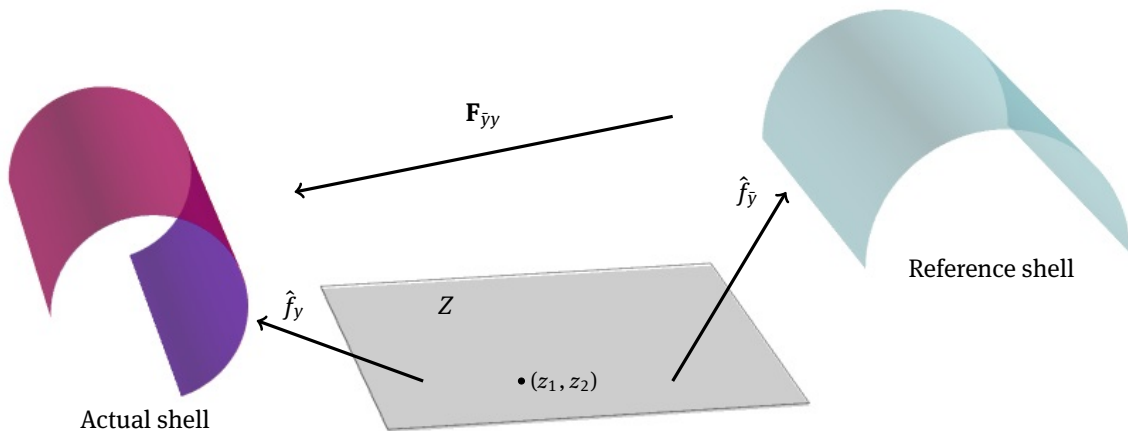


Figure 2: Given a flat computational domain Z , the map $\hat{f}_{\bar{y}} : Z \rightarrow \mathcal{E}$ defines a reference shell. The actual shell $\hat{f}_{\bar{y}} : Z \rightarrow \mathcal{E}$ is the unknown of our problem; the configuration $\hat{f}_{\bar{y}}$ is found by assigning a target metric. The map $\mathbf{F}_{\bar{y}y}$ is the deformation of $\hat{f}_{\bar{y}}$ with respect to $\hat{f}_{\bar{y}}$.

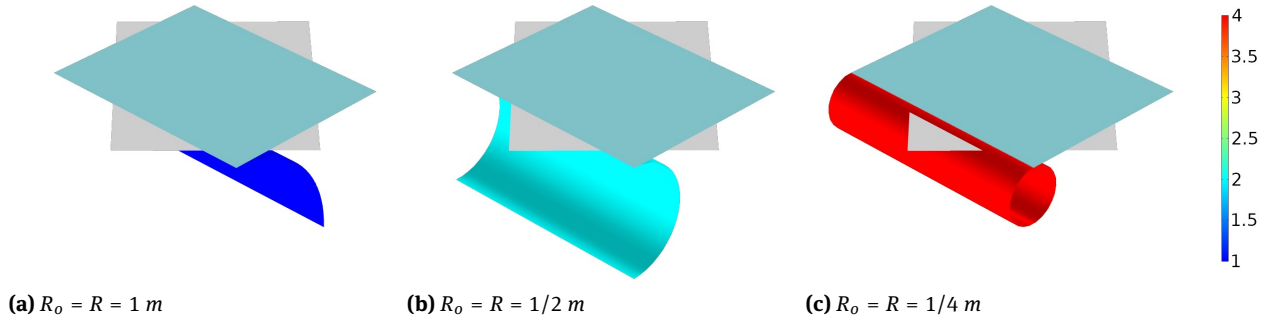


Figure 3: Bending of a flat shell obtained by a change of the target metric \mathbf{B}_o . Each of the three plots shows the computational domain (gray), the reference surface (cyan), and the actual shape (color map of curvature). Each deformed configuration is stress-free.

representation $[\hat{f}_y]$ of \hat{f}_y is given by the map

$$[\hat{f}_y] = \begin{bmatrix} z_1 \cos(\pi/4) - z_2 \sin(\pi/4) \\ z_1 \sin(\pi/4) + z_2 \cos(\pi/4) \\ 0 \end{bmatrix}. \quad (40)$$

In this example \hat{f}_y is a rigid motion, and equations (36) hold. The shell is clamped along one edge, and free at the remaining edges. We impose an increasing bending distortion \mathbf{B}_o at constant target stretch \mathbf{A}_o , by assigning the following target FFs:

$$\mathbf{A}_o = \begin{bmatrix} 1 & 0 \\ 0 & 1 \end{bmatrix}, \quad \mathbf{B}_o = \begin{bmatrix} 1/R_o & 0 \\ 0 & 0 \end{bmatrix}. \quad (41)$$

Given (41), also (37) hold; the FFs are compatible, and any deformed configuration will be stress-free; from (30) and (36, 37) it follows

$$\mathbf{E}_{e0} = \frac{1}{2}(\mathbf{A}_y - \mathbf{I}), \quad \mathbf{E}_{e1} = \mathbf{B}_y - \text{sym}(\mathbf{A}_y \mathbf{B}_o). \quad (42)$$

The elastic energy has a minimum for $\mathbf{A}_y = \mathbf{I}$ and $\mathbf{E}_{e1} = 0$; this last condition yields

$$0 = \frac{1}{R} - \frac{1}{R_o} \quad \Rightarrow \quad R = R_o. \quad (43)$$

Thus, the actual configuration lies on a cylinder with radius R_o . In this example we set $L = \pi/2 \text{ m}$; thus, the flat shell will become a cylinder when the actual curvature radius $R = L/(2\pi) = 1/4 \text{ m}$. We solve a sequence of elastic problems with the target curvature radius R_o running from $R_o \gg 1 \text{ m}$, corresponding to an almost undeformed configuration, to $R_o = 1/4 \text{ m}$, corresponding to the closed cylinder. Three solutions of this morphing problem are shown in Figure 3.

4.2 Bending at constant stretch (cylindrical reference)

We consider as reference shell \hat{f}_y , a shell having the shape of half cylinder, with axis parallel to \mathbf{c}_2 ; the matrix-like

representation $[\hat{f}_y]$ of \hat{f}_y is given by the map

$$[\hat{f}_y] = \begin{bmatrix} R_c \sin(z_1/R_c) \\ z_2 \\ R_c \cos(z_1/R_c) \end{bmatrix}, \quad (44)$$

with R_c the curvature radius of the reference shell. The shell is clamped along one edge, and free at the remaining edges. We impose an increasing bending distortion \mathbf{B}_o at constant target stretch \mathbf{A}_o , by assigning the following target FFs:

$$\mathbf{A}_o = \begin{bmatrix} 1 & 0 \\ 0 & 1 \end{bmatrix}, \quad \mathbf{B}_o = \begin{bmatrix} 1/R_o & 0 \\ 0 & 0 \end{bmatrix}. \quad (45)$$

For this example the FFs in (41) are compatible, and any deformed configuration will be stress-free; as equations (38) hold, the elastic energy has a minimum when

$$\begin{aligned} \mathbf{E}_{e0} &= \frac{1}{2}(\mathbf{A}_y - \mathbf{I}) = 0, \\ \mathbf{E}_{e1} &= \mathbf{B}_y - \text{sym}(\mathbf{A}_y(\mathbf{B}_y + \mathbf{B}_o)) = 0. \end{aligned} \quad (46)$$

The minimum condition yields $\mathbf{A}_y = \mathbf{I}$ and $\mathbf{E}_{e1} = 0$; it follows

$$\frac{1}{R} = \frac{1}{R_c} + \frac{1}{R_o} \quad \Rightarrow \quad R = \frac{R_c R_o}{R_c + R_o}, \quad R_o = \frac{R_c R}{R_c - R}. \quad (47)$$

Thus, the actual configuration lies on a cylinder with radius R . In this example we set $L = \pi/2 \text{ m}$, $R_c = 1/2 \text{ m}$, and the reference half cylinder will become a cylinder when the actual curvature radius $R = 1/4 \text{ m}$. We solve a sequence of elastic problems with the target curvature radius R_o running from $R_o \gg 1 \text{ m}$, corresponding to an almost undeformed configuration, to $R_o = 1/2 \text{ m}$, corresponding to a closed cylinder. Three solutions of this morphing problem are shown in Figure 4.

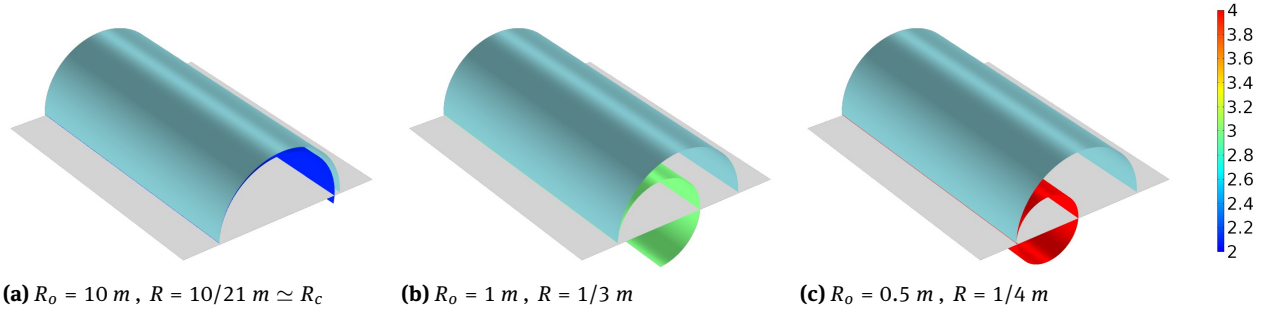


Figure 4: Bending of a cylindrical shell obtained by a change of the target metric \mathbf{B}_o . Each of the three figures shows the computational domain (gray), the reference surface (cyan), and the actual shape (color map of curvature). Each deformed configuration is stress-free.

4.3 Bending at constant stretch (cylinder with slide)

We consider as reference shell $\hat{f}_{\bar{y}}$, the same shell of the previous example, see (44). The shell is pinned along one edge, and has a slide constraint on the opposite edge; we impose a bending distortion at constant stretch; the target FFs \mathbf{A}_o , \mathbf{B}_o are given by

$$\mathbf{A}_o = \begin{bmatrix} 1 & 0 \\ 0 & 1 \end{bmatrix}, \quad \mathbf{B}_o = \begin{bmatrix} 1/R_o & 0 \\ 0 & 0 \end{bmatrix}. \quad (48)$$

The FFs in (48) are compatible, (46) holds, and the solutions of this example coincide with the solutions of the previous one, but a rigid motion. In this example $L = \pi/2$ m; the curvature radius R_o runs from $R_o \gg 1$ m, corresponding to an almost undeformed configuration, to $R_o = 0.6$ m. Three solutions of this morphing problem are shown in Figure 5.

4.4 Stretching at constant curvature (cylindrical reference)

We consider as reference shell $\hat{f}_{\bar{y}}$, a shell having the shape of half cylinder, with axis parallel to \mathbf{c}_2 ; the matrix-like representation $[\hat{f}_{\bar{y}}]$ of $\hat{f}_{\bar{y}}$ is given by the map

$$[\hat{f}_{\bar{y}}] = \begin{bmatrix} R_c \sin(z_1/R_c) \\ z_2 \\ R_c \cos(z_1/R_c) \end{bmatrix}, \quad (49)$$

The shell is clamped along one edge, and free at the remaining ones. We assign a membrane distortion at constant curvature; the target FFs \mathbf{A}_o , \mathbf{B}_o are given by

$$\mathbf{A}_o = \begin{bmatrix} \lambda^2 & 0 \\ 0 & 1 \end{bmatrix}, \quad \mathbf{B}_o = \begin{bmatrix} 1/R_o & 0 \\ 0 & 0 \end{bmatrix}, \quad (50)$$

where λ is a parameter measuring the membrane stretch. The FFs in (50) are compatible, any deformed configuration will be stress-free, and the elastic energy has a minimum

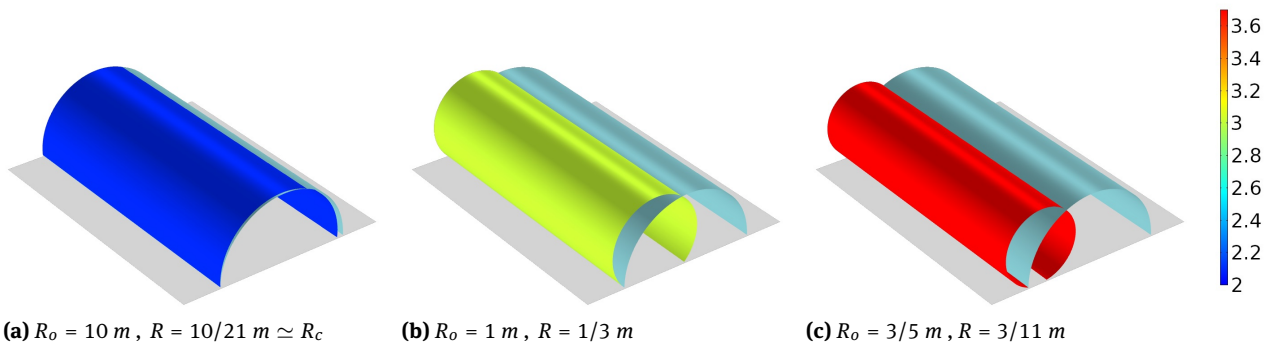


Figure 5: Bending of a cylindrical shell obtained by a change of the target metric \mathbf{B}_o ; edge at left is pinned, edge at right has a slide. Each of the three figures shows the computational domain (gray), the reference surface (cyan), and the actual shape (color map of curvature). Each deformed configuration is stress-free.

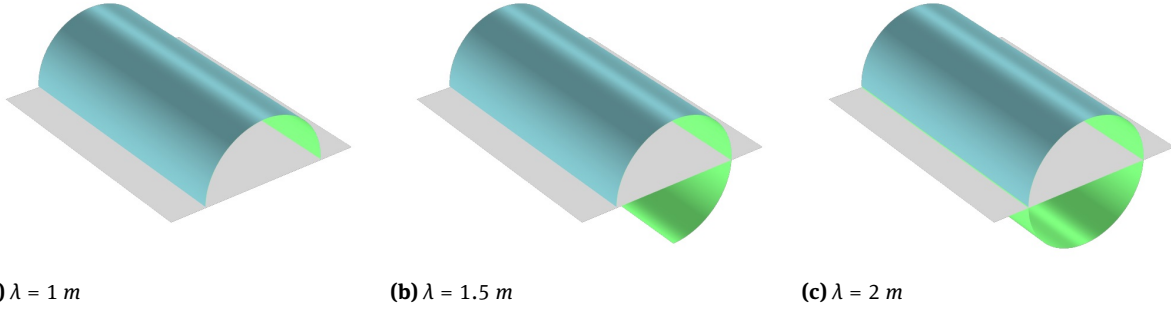


Figure 6: Effects of the membrane distortion at constant curvature of a cylindrical shell. Each of the three figures shows the computational domain (gray), and the actual surface (cyan up and green at bottom) for three different values of the stretch λ . Each deformed configuration is stress-free.

when $\mathbf{E}_{e0} = 0$ and $\mathbf{E}_{e1} = 0$. This minimum condition yields

$$\begin{aligned} \mathbf{A}_{\bar{y}y} &= \mathbf{U}_{\bar{y}0}^{-1} \mathbf{A}_y \mathbf{U}_{\bar{y}0}^{-1} = \mathbf{A}_o, \\ \mathbf{B}_{\bar{y}y} &= \mathbf{U}_{\bar{y}0}^{-1} \left(\mathbf{B}_y - \text{sym}(\mathbf{A}_y \mathbf{U}_{\bar{y}0}^{-1} \mathbf{U}_{\bar{y}1}) \right) \mathbf{U}_{\bar{y}0}^{-1} = \mathbf{B}_o = \text{const}, \end{aligned} \quad (51)$$

which implies, being $\mathbf{U}_{\bar{y}0} = \mathbf{I}$, $\mathbf{U}_{\bar{y}1} = \mathbf{B}_{\bar{y}}$, the following conditions

$$\mathbf{A}_y = \mathbf{A}_o, \quad \mathbf{B}_y - \text{sym}(\mathbf{A}_o \mathbf{B}_{\bar{y}}) = \mathbf{B}_o. \quad (52)$$

We assume a trial solution $\hat{f}_{\bar{y}}$ having the same form of (49), and we compute the associated FFs by using (11); we have

$$\begin{aligned} [\hat{f}_{\bar{y}}] &= \begin{bmatrix} R \sin(\delta z_1/R) \\ z_2 \\ R \cos(\delta z_1/R) \end{bmatrix}, \quad \mathbf{A}_y = \begin{bmatrix} \delta^2 & 0 \\ 0 & 1 \end{bmatrix}, \\ \mathbf{B}_y &= \begin{bmatrix} \delta^2/R & 0 \\ 0 & 0 \end{bmatrix}. \end{aligned} \quad (53)$$

From (50), (52), it follows $\delta = \lambda$, and

$$\frac{\lambda^2}{R} = \frac{1}{R_o} + \frac{\lambda^2}{R_c}. \quad (54)$$

We set $R_o \rightarrow \infty$; it follows that any actual configuration lies on a cylinder with radius $R = R_c$; with $L = \pi R_c$, $R_c = 1/2$ m, we obtain a closed cylinder with $\lambda = 2$. Three different configurations are shown in Figure 6.

4.5 Curling (flat reference)

Here, we curl a flat shell by imposing a curvature which depends on the z_1 coordinate. We consider as reference shell $\hat{f}_{\bar{y}}$ the reference domain; the matrix-like representation $[\hat{f}_{\bar{y}}]$ of $\hat{f}_{\bar{y}}$ is given by the map

$$[\hat{f}_{\bar{y}}] = \begin{bmatrix} z_1 \\ z_2 \\ 0 \end{bmatrix}, \quad (55)$$

The shell is clamped along one edge, and free at the remaining ones. The curling is achieved by imposing the following FFs:

$$\mathbf{A}_o = \begin{bmatrix} 1 & 0 \\ 0 & 1 \end{bmatrix}, \quad \mathbf{B}_o = \begin{bmatrix} 1/R_o(z_1) & 0 \\ 0 & 0 \end{bmatrix}, \quad (56)$$

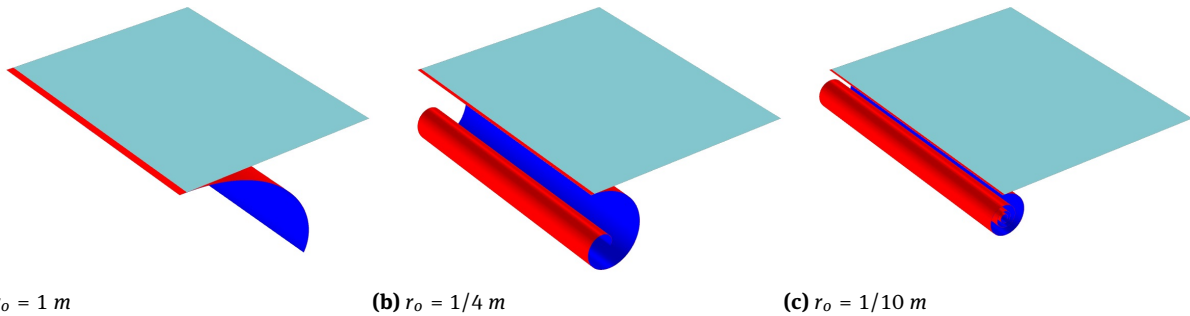


Figure 7: Effects of the non-homogeneous bending distortion for a flat shell. Each of the three figures shows the reference surface (cyan), which in this case coincides with the computational domain, and the actual surface (red up and blue at bottom) for three different values of the parameter r_o . Each deformed configuration is stress-free.

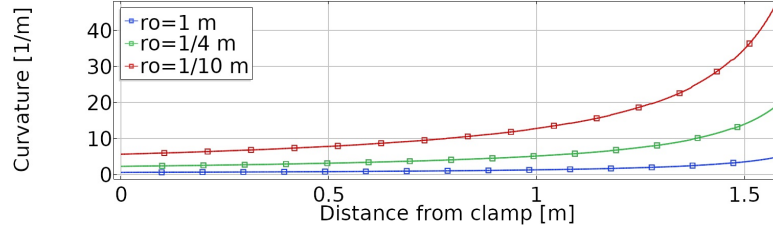


Figure 8: Curvature versus Distance from clamp for three different values of the parameter r_o . The numerical solutions (markers) equal the explicit solution (solid line) given by (58).

with $R_o(z_1) = r_o(1 - z_1/1[m])$. Given (56), equations (36, 38) hold; the FFs are compatible, and any deformed configuration will be stress-free; the condition that minimizes the elastic energy is:

$$\mathbf{E}_{e0} = \frac{1}{2} (\mathbf{A}_y - \mathbf{I}) = 0, \quad (57)$$

$$\mathbf{E}_{e1} = \mathbf{B}_y - \text{sym}(\mathbf{A}_y(\mathbf{B}_y + \mathbf{B}_o)) = 0.$$

It follows $\mathbf{A}_y = \mathbf{I}$; moreover, being the reference shell flat, we have $\mathbf{B}_y = 0$, and the actual curvature is equal to the target one:

$$\frac{1}{R(z_1)} = \frac{1}{R_o(z_1)}. \quad (58)$$

Three configurations corresponding to different values of r_o are shown in Figure 7; in Figure 8 we benchmark the explicit curvature against the curvature computed from the numerical solution.

4.6 Twist of a flat shell

We morph a flat shell by imposing an uniaxial distortion, described by two parameters, the stretch Λ_{\parallel} , and the orientation θ of the distortion axis with respect to the bar axis. We consider as reference shell \hat{f}_y the reference domain with aspect ratio $L/W = 10$; the matrix-like representation $[\hat{f}_y]$ of \hat{f}_y is given by the map

$$[\hat{f}_y] = \begin{bmatrix} z_1 \\ z_2 \\ 0 \end{bmatrix}. \quad (59)$$

The twisting is achieved by imposing the following FFs:

$$\mathbf{A}_o = \Lambda^+ \begin{bmatrix} 1 & 0 \\ 0 & 1 \end{bmatrix} + \Lambda^- a \begin{bmatrix} \cos(2\theta) & \sin(2\theta) \\ \sin(2\theta) & \cos(2\theta) \end{bmatrix}, \quad (60)$$

$$\mathbf{B}_o = \frac{3}{H} b \Lambda^- \begin{bmatrix} \sin(2\theta) & \cos(2\theta) \\ \cos(2\theta) & \sin(2\theta) \end{bmatrix},$$

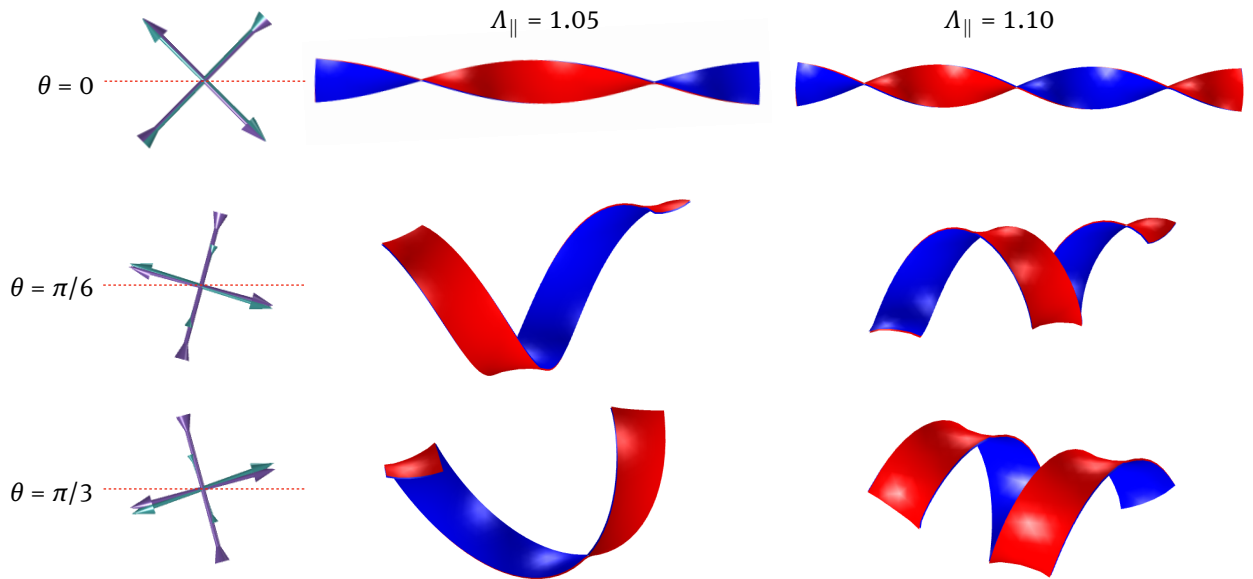


Figure 9: Twist of a flat shell. Each row shows, from left to right: 1) the eigenvectors of \mathbf{B}_y (green) and \mathbf{B}_o (violet) against the axis of the reference domain (red, dashed line); 2) The actual configuration for $\Lambda = 1.05$; 3) The actual configuration for $\Lambda = 1.10$. To highlight the ribbon-like shape, the two sides of the actual shape have different colors (blue and red). The eigenvectors correspond to $\Lambda = 1.10$; their misalignment is a clue about the incompatibility of the target metric. We note that also the eigenvalues of \mathbf{B}_y and \mathbf{B}_o are different.

with

$$\Lambda^+ = \frac{\Lambda_{\parallel} + \Lambda_{\perp}}{2}, \Lambda^- = \frac{\Lambda_{\parallel} - \Lambda_{\perp}}{2}, \Lambda_{\perp} = \frac{1}{\sqrt{\Lambda_{\parallel}}}, \quad (61)$$

$$a = \frac{\sin(\gamma)}{\gamma}, b = \frac{\sin(\gamma) - \gamma \cos(\gamma)}{\gamma^2}.$$

We set $\gamma = \pi/2$. The FFs (60) are not compatible, and any deformed configuration will be stressed; to minimize the reaction to the constraints, we fix the displacements of the point $z_1 = 0 \text{ m}, z_2 = 10^{-4} \text{ m}$ along z_1 and z_2 and those of the point $z_1 = 0 \text{ m}, z_2 = 0 \text{ m}$ along the directions z_1 and z_3 , respectively. We run a parametric analysis with $\theta = 0, \pi/3, 2\pi/3$, and $\Lambda_{\parallel} \in (1, 1.1)$; six solutions of this morphing problem are shown in Figure 9.

5 Conclusions

This work presents a new method for morphing shell-like bodies. The morphing is obtained by assigning a distortion field, which in turns, induces a target metric: the actual configuration will minimize the elastic energy, measuring the distance between the target metric and the actual one. This procedure could be useful in computer graphics and shape analysis, for example in physics-based modeling and character animation for the movie industry. We note that the proposed technique may be used to the full hierarchy of geometric manifolds, that is, for 1D curves, 2D surfaces, and 3D solids, provided the appropriate metric information is used.

We provided some simple, yet non trivial, examples to demonstrate the effectiveness of the procedure; we also defined an error function to measure the metric gap between the assigned target metric and the metric realized by the embedding. The numerical experiments clearly show good results, and the method is able to transport compatible metric changes, even in the presence of very different geometries. The error function shows that the lack of compatibility is localized in a small portion of the manifold, where very large deformations need to be realized to meet the demands of the target metric. The presence of this errors seems to not affect the global performance of the method.

Funding information: This work is supported by MIUR (Italian Minister for Education, Research, and University) through *PRIN 2017, Mathematics of active materials: From mechanobiology to smart devices*, project n. 2017KL4EF3. The authors also acknowledge the support of the Italian Group of Mathematical Physics (GNFM-INdAM).

Author contributions: All authors have accepted responsibility for the entire content of this manuscript and approved its submission.

Conflict of Interests: The authors state no conflict of interest.

References

- [1] Chern A, Knöppel F, Pinkall U, Schröder P. Shape from metric. *ACM Trans. Graph.* 2018;37(4):63:1–17.
- [2] Boscaini D, Eynard D, Kourounis D, Bronstein MM. Shape-from-Operator: Recovering Shapes from Intrinsic Operators. *Comput Graph Forum.* 2015;34(2):265–74.
- [3] Lembo M. On the determination of deformation from strain. *Mechanica.* 2017;52(9):2111–25.
- [4] Pietraszkiewicz W, Szwabowicz M, Vallée C. Determination of the midsurface of a deformed shell from prescribed surface strains and bendings via the polar decomposition. *Int J Non-linear Mech.* 2008;43(7):579–87.
- [5] Klein Y, Efrati E, Sharon E. Shaping of elastic sheets by prescription of non-Euclidean metrics. *Science.* 2007 Feb;315(5815):1116–20.
- [6] Nardinocchi P, Teresi L, Varano V. The elastic metric: A review of elasticity with large distortions. *Int J Non-linear Mech.* 2013;56:34–42.
- [7] Ciarlet PG. *An Introduction to Differential Geometry with Applications to Elasticity.* Springer. 2005.
- [8] Teresi L, Milicchio F, Gabriele S, Piras P, Varano V. Shape deformation from metric's transport. *Int J Non-linear Mech.* 2020;119.
- [9] Abdelmohsen S, Adriaenssens S, El-Dabaa R, Gabriele S, Olivieri L, Teresi L. A multi-physics approach for modeling hygroscopic behavior in wood low-tech architectural adaptive systems. *CAD Comput. Aided Des.* 2019;106:43–53.
- [10] Adriaenssens S, Block P, Veenendaal D, Williams C. *Shell structures for architecture: Form finding and optimization.* Routledge. 2014.
- [11] Laccone F, Malomo L, Pérez J, Pietroni N, Ponchio F, Bickel B, Cignoni P. A bending active twisted-arch plywood structure: computational design and fabrication of the flex maps pavilion. *SN Appl. Sci.* 2020;2(9).
- [12] Kröner E. Allgemeine kontinuumstheorie der versetzungen und eigenspannungen. *Arch Ration Mech Anal.* 1959;4(1):273–334.
- [13] Lee E. Elastic-plastic deformation at finite strains. *J Appl Mech.* 1969;36(1):1–6.
- [14] Davini C. Some remarks on the continuum theory of defects in solids. *Int J Solids Struct.* 2001;38(6-7):1169–82.
- [15] Koiter W. On the nonlinear theory of thin elastic shells, in: *Proc. K. Ned. Akad. Wet.* 1966;B 69:1–54.
- [16] Sneddon IN, Hill R, Naghdi PM, Ziegler H. *Progress in solid mechanics.* Amsterdam, New York: John Wiley & Sons. 1963;4.

A The Shell model

We summarize the shell model used in our analyses, a model derived from the Naghdi-Shell model [16] which includes a constraint on the out-of plane shear.

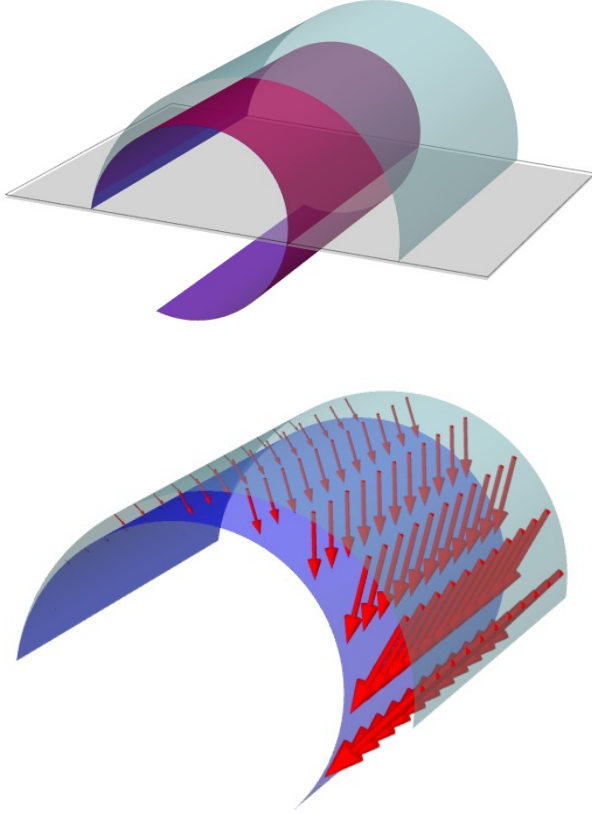


Figure A1: Top. Computational domain Ω (gray), reference surface $\hat{f}_y(\Omega)$ (cyan) and actual surface $\hat{f}_y(\Omega)$ (red). Bottom. Displacement field $\mathbf{u} = \hat{f}_y - \hat{f}_y$ (red arrows), represented as a spatial field $\mathbf{u} = \mathbf{u}(\hat{f}_y(\Omega))$.

A.1 State variables

Given the orthonormal frame $\{o, \mathbf{c}_1, \mathbf{c}_2, \mathbf{c}_3\}$, let $\Omega \in \text{span}(\mathbf{c}_1, \mathbf{c}_2)$ be a flat, 2D domain. The surface $\hat{f}_y : \Omega \rightarrow \mathcal{E}$ is our reference shell, while the surface $\hat{f}_y : \Omega \rightarrow \mathcal{E}$ is the actual shell shape, and represents the unknown of our problem, see Figure A1, top. Given the source shell $f_y = \hat{f}_y + \zeta \mathbf{n}_y$, using (7) we define the moving frame $\{\mathbf{e}_1, \mathbf{e}_2, \mathbf{n}_y\}$, composed of the unit tangent vectors \mathbf{e}_α and the normal vector

\mathbf{n}_y :

$$\mathbf{e}_1 = \frac{\mathbf{a}_{y1}}{\|\mathbf{a}_{y1}\|}, \quad \mathbf{e}_2 = \frac{\mathbf{a}_{y2}}{\|\mathbf{a}_{y2}\|}, \quad \mathbf{n}_y = \mathbf{e}_1 \times \mathbf{e}_2; \quad (\text{A1})$$

The state variables of the model comprehend three kinematical fields, displacement, rotation and shear, plus a dynamical field, the shear stress:

$$\begin{aligned} \mathbf{u} &= u_1 \mathbf{e}_1 + u_2 \mathbf{e}_2 + u_3 \mathbf{n}_y && \text{displacements;} && (\text{A2}) \\ \beta &= (\beta_1, \beta_2) && \text{rotation parameters;} \\ \gamma &= (\gamma_1, \gamma_2) && \text{shear stretch;} \\ \tau &= (\tau_1, \tau_2) && \text{shear stress.} \end{aligned}$$

Then, the target shell $f_y = \hat{f}_y + \zeta \mathbf{n}_y$ is described by displacing \hat{f}_y along $\mathbf{e}_1, \mathbf{e}_2, \mathbf{n}_y$ with

$$\hat{f}_y = \hat{f}_y + \mathbf{u}, \quad (\text{A3})$$

see Figure A1, bottom. We define the normal \mathbf{d} to the actual surface in terms of the state variable β_α through a rotation $\mathbf{R}(\beta_\alpha)$ of the moving frame, and the shear deformation γ_d in terms of \mathbf{d} as follows

$$\mathbf{d} = \mathbf{R}(\beta_1, \beta_2) \{\mathbf{e}_1, \mathbf{e}_2, \mathbf{n}_y\}, \quad \gamma_d = \hat{\mathbf{F}}_y^T \mathbf{d}. \quad (\text{A4})$$

Denoting with e_{aj}, n_{yj} the Cartesian component of the moving frame $\{\mathbf{e}_1, \mathbf{e}_2, \mathbf{n}_y\}$, the Cartesian components of d_j are given by

$$\begin{aligned} d_1 &= (\sin \beta_1 e_{21} + \cos \beta_1 n_{y1}) \cos \beta_2 + \sin \beta_2 e_{11}, && (\text{A5}) \\ d_2 &= (\sin \beta_1 e_{22} + \cos \beta_1 n_{y2}) \cos \beta_2 + \sin \beta_2 e_{12}, \\ d_3 &= (\sin \beta_1 e_{23} + \cos \beta_1 n_{y3}) \cos \beta_2 + \sin \beta_2 e_{13}. \end{aligned}$$

Analogously, the two components of γ_d are given by

$$\gamma_{d\alpha} = \mathbf{a}_{y\alpha} \cdot \mathbf{d} \quad \text{with} \quad a_{y\alpha} = \hat{f}_{y,\alpha} \Rightarrow \gamma_d = \hat{\mathbf{F}}_y^T \mathbf{d}. \quad (\text{A6})$$

The second fundamental form \mathbf{B}_y is then computed by using the gradient of \mathbf{d} : $\mathbf{B}_y = \nabla \mathbf{d}^T \hat{\mathbf{F}}_y$.

A.2 The elastic energy

We assume the elastic energy density ψ , a density per unit distorted area, to be the sum of three contributions, a membrane energy ψ_m , a bending energy ψ_b and a shear energy ψ_γ :

$$\psi = (\psi_m(\mathbf{E}_{e0}) + \psi_b(\mathbf{E}_{e1}) + \psi_\gamma(\gamma)) J_o J_y \quad (\text{A7})$$

Here, J_o measure the relative area change between the distorted area-element and the reference area-element

$$J_o = \sqrt{\det \mathbf{A}_o} = \det \mathbf{U}_o, \quad (\text{A8})$$

and $J_{\tilde{y}} = \det(\mathbf{U}_{\tilde{y}})$. The three energy densities are defined as:

$$\begin{aligned}\psi_m(\mathbf{E}_{e0}) &= \mu_1 \operatorname{tr}(\mathbf{E}_{e0})^2 + \mu_2 \operatorname{tr}(\mathbf{E}_{e0}^2), \\ \psi_b(\mathbf{E}_{e1}) &= b_1 \operatorname{tr}(\mathbf{E}_{e1})^2 + b_2 \operatorname{tr}(\mathbf{E}_{e1}^2), \\ \psi_\gamma(\gamma) &= \frac{1}{2} \mu_2 \gamma \cdot \gamma.\end{aligned}\quad (\text{A9})$$

We note that the target fundamental forms enter into the membrane and bending energies through the strains \mathbf{E}_{e0} and \mathbf{E}_{e1} , see (33). In the framework of mixed methods, we require the shear variable γ to be equal to the shear deformation γ_d , that is, we introduce the shear constraint $\gamma = \gamma_d$; it follows that the dynamical state variable τ must be considered as the shear-stress reaction enforcing such a kinematical constraint. Then, we relax the energy ψ by considering the work done by the shear stress on the shear constraint

$$\psi_r = \psi_m(\mathbf{E}_{e0}) + \psi_b(\mathbf{E}_{e1}) + \psi_\gamma(\gamma) - \tau \cdot (\gamma - \gamma_d). \quad (\text{A10})$$

The variation of ψ_r identifies the elastic dynamical-actions as derivatives of the energy with respect to the elastic strains

$$\begin{aligned}\tilde{\psi}_r &= \underbrace{\frac{\partial \psi_m(\mathbf{E}_{e0})}{\partial \mathbf{E}_{e0}}}_{\mathbf{s}_{e0}} \cdot \tilde{\mathbf{E}}_{e0} + \underbrace{\frac{\partial \psi_b(\mathbf{E}_{e1})}{\partial \mathbf{E}_{e1}}}_{\mathbf{s}_{e1}} \cdot \tilde{\mathbf{E}}_{e1} \\ &+ \underbrace{\left(\frac{\partial \psi_\gamma(\gamma)}{\partial \gamma} - \tau \right)}_{\boldsymbol{\tau}_e} \cdot \tilde{\gamma} + \tau \cdot \tilde{\gamma}_d - \tilde{\tau} \cdot \underbrace{(\gamma - \gamma_d)}_{\text{constraint}}.\end{aligned}\quad (\text{A11})$$

The solution of the problem satisfies the following balance equation in weak form:

$$\tilde{\psi}_r = 0, \quad \forall \tilde{\mathbf{u}}, \tilde{\boldsymbol{\beta}}, \tilde{\gamma}, \tilde{\tau} \quad (\text{A12})$$

compatible with the boundary conditions.

It is worth noting that, given (30), (32)₂, $\tilde{\mathbf{E}}_{e0}$ contains the variation of both \mathbf{A}_y and \mathbf{B}_y ; in turns, being $\mathbf{B}_y = \nabla \mathbf{d}^T \hat{\mathbf{F}}_y$, it follows that $\tilde{\mathbf{B}}_y$ contains variations of \mathbf{d} and $\hat{\mathbf{F}}_y$.

A.3 The stiffness parameters

The shell stiffnesses are given in terms of the Lamé parameters λ and μ as follows. The membrane stiffnesses μ_i are defined by

$$\mu_1 = h \frac{\lambda \mu}{\lambda + 2 \mu}, \quad \mu_2 = h \mu; \quad (\text{A13})$$

the bending stiffnesses b_i are given by

$$b_1 = \frac{h^3}{12} \frac{\lambda \mu}{\lambda + 2 \mu}, \quad b_2 = \frac{h^3}{12} \mu. \quad (\text{A14})$$

We note that introducing the bulk modulus $k = \lambda + 2/3 \mu$, we can write the stiffness in μ_1 and b_1 as a function of μ , k

$$\frac{\lambda \mu}{\lambda + 2 \mu} = \frac{(3k - 2\mu)\mu}{3k + 4\mu}. \quad (\text{A15})$$

It is worth noting the importance of the values of the elastic moduli; in particular for isotropic material it is important the ratio k/μ between the bulk and the shear modulus. In our examples we used $k/\mu \sim 1$. In our computations, we used the values for the Lamé parameters: $\lambda = 1.5\text{N/m}^2$, and $\mu = 1\text{N/m}^2$.